are near linear (**1**, U(1)-N(3)-Si(4) = 178.3 (11)°; **2**, U(1)-N-(3)-C(4) = 173.5 (7)°). In the case of $(MeC_5H_4)_3U(NPh)$, this linearity has been described as an indication of multiple bonding between uranium and nitrogen, with both lone pairs of the nitrogen being donated into e symmetry metal atomic orbitals to form a U≡N triple bond.[14,16] This bonding scheme also explains the unusually short uranium-imide nitrogen bond lengths. The latter range from 2.02 to 2.07 Å in the tris(cyclopentadienyl)uranium complexes,[14-16] while $[(Me_3Si)_2N]_3U(NSiMe_3)$ displays a U-N (imide) bond length of 1.910 (16) Å.[5a] Oxidation to U(VI) should remove the final electron from a nonbonding f orbital, but one would expect a slight shortening of the U-N bond length due to the relative radii of U(V) and U(VI). The bond length U(1)-N(3) in complex **1** is 1.854 (23) Å, while in **2** this bond distance is 1.979 (8) Å. Within the error limits, there appears to be no significant difference in the metal-imide nitrogen bond lengths between the U(V) and U(VI) complexes. We believe this to be a reflection of the steric crowding about the metal center in the uranium(VI) systems. This crowding may also be the origin of the difference in U-N (imide) bond lengths between complexes **1** and **2**. The N(3)-Si(4) bond length (1.824 (24) Å) in **1** is substantially longer than the N(3)-C(4) bond length (1.392 (12) Å) in **2**. This decreases the steric demand of the imido ligand in **1**. The U-F bond lengths in **1** and **2** are 2.013 (12) and 2.068 (5) Å, respectively. For comparison, the mean U-F bond length in $UF_6$ is 1.995 (3) Å.[17]

Steric crowding about the uranium(VI) centers is also reflected in the solution behavior of the complexes. At room temperature, the $^1H$ NMR spectra of both monomers indicate a static structure, in which rotation about the equatorial U-N bonds is restricted, giving rise to inequivalent trimethylsilyl amide resonances. Upon warming, these resonances broaden and coalesce (60 °C for complex **1**, 55 °C for complex **2**). Continued heating results in the decomposition of the uranium(VI) complexes and the appearance of resonances due to *reduced* pyrolysis products. This solution decomposition also takes place over the course of several days at room temperature.

One unusual feature of the $^1H$ NMR spectrum of **2** is the location of the imido phenyl proton resonances at $\delta$ 9.06 (meta), 2.03 (ortho), and -0.28 (para). These resonances do not shift between -75 and +50 °C in toluene-$d_8$ and are observed at room temperature in THF-$d_8$. We offer two possible explanations for this behavior: (1) a high degree of ionic character in the metal-imide nitrogen bond is resonance delocalized to the ortho and para carbons, which, in turn, shields the attached protons and shifts them to higher field, and/or (2) the uranium(VI) ion is a temperature-independent paramagnet (TIP). The latter behavior has been observed in several uranyl complexes.[18-21] Attempts to measure a (presumably) small TIP for solids **1** and **2** have been hampered by their thermal instability.

In summary, the first examples of uranium(VI) complexes with a multiple bond to a main-group element other than oxygen have been synthesized and structurally characterized. Whether uranium(VI) can be stabilized by multiply bonded ligands other than imido and oxo remains to be determined. We are presently operating under the assumption that, with the correct choice of ancillary ligands, uranium(VI) will support nitrido and perhaps even alkylidene and alkylidyne ligands in its coordination sphere.

**Acknowledgment.** We thank Dr. W. G. Van Der Sluys and Dr. D. L. Clark (LANL) for helpful discussions and Dr. M. W. McElfresh, IBM T. J. Watson Research Center, for his attempts to measure the solid-state magnetic properties of **1** and **2**. C.J.B. is the recipient of a J. Robert Oppenheimer Fellowship at Los Alamos. The work was performed under the auspices of the Division of Chemical Sciences, Office of Energy Research, U.S. Department of Energy.

**Supplementary Material Available:** Tables of crystal data, atomic positional parameters, anisotropic thermal parameters, and selected bond lengths and angles for **1** and **2** (16 pages); tables of observed and calculated structure factors for **1** and **2** (22 pages). Ordering information is given on any current masthead page.

(16) Cramer, R. E.; Edelmann, F.; Mori, A. L.; Roth, S.; Gilje, J. W.; Tatsumi, K.; Nakamura, A. *Organometallics* **1988**, *7*, 841.
(17) Levy, J. H.; Taylor, J. C.; Wilson, P. W. *J. Chem. Soc., Dalton Trans.* **1976**, 219.
(18) Eisenstein, J. C.; Pryce, M. H. L. *Proc. R. Soc. London, A* **1960**, *229*, 20.
(19) McGlynn, S. P.; Smith, J. K. *J. Mol. Spectrosc.* **1962**, *6*, 164.
(20) Denning, R. G.; Norris, J. O. W.; Short, I. G.; Snellgrove, T. R.; Woodmark, D. R. *ACS Symp. Ser.* **1980**, *No. 131*, 313.
(21) Denning, R. G.; Snellgrove, T. R.; Woodmark, D. R. *Mol. Phys.* **1979**, *37*, 1109.

## Spontaneously Formed Functionally Active Avidin Monolayers on Metal Surfaces: A Strategy for Immobilizing Biological Reagents and Design of Piezoelectric Biosensors

Richard C. Ebersole, Jeffrey A. Miller, John R. Moran, and Michael D. Ward*

*Contribution No. 5382*
*Central Research and Development Department*
*E. I. du Pont de Nemours and Co., Experimental Station*
*P.O. Box 80328, Wilmington, Delaware 19880-0328*

*Received December 20, 1989*

Immobilization of biologically relevant entities for diagnostic assays[1-4] has been widely studied on polymeric and oxide supports. Immobilization on metallic surfaces, however, has not been investigated extensively. Such methodology is important for the design of electronic diagnostic sensors in which the transducing elements commonly include a metallic electrode, such as in electrochemical and piezoelectric devices. We report a novel strategy for immobilizing biological reagents on metallic surfaces and demonstrate its use in a DNA hybridization assay.

We find that robust, functionally active monolayers of avidin and streptavidin form spontaneously, *and irreversibly*, from aqueous solutions onto freshly evaporated gold and silver surfaces.[5] The ellipsometrically determined thicknesses were $d$(avidin) = 48 Å and $d$(streptavidin) = 42 Å, consistent with the presence of protein monolayers as inferred from the crystal structure of streptavidin.[6] The monolayers form rapidly (<10 min) under a wide range of conditions. Varying the NaCl concentration (0.1-1 M) or pH (3-11) had little effect on monolayer formation. The observation that both proteins form monolayers indicates that metal-sulfur interactions via cysteine residues are not a dominant factor, since cysteine is present in avidin but absent in streptavidin. The pI values for avidin and strepavidin are 10 and ca 7, respectively;[7,8] therefore, the absence of a pH effect indicates that

(1) Wilchek, M.; Bayer, E. A. *Anal. Biochem.* **1988**, *171*, 1-32.
(2) Henrikson, K. P.; Allen, S. H. G.; Maloy, W. L. *Anal. Biochem.* **1979**, *94*, 366-370.
(3) Gould, E. A.; Buckley, A.; Cammack, N. *J. Virol. Methods* **1985**, *11*, 41-48.
(4) Leary, J. J.; Brigati, D. J.; Ward, D. C. *Proc. Natl. Acad. Sci. U.S.A.* **1983**, *80*, 4045-4049.
(5) Gold and silver films (2000 Å) with chromium underlayers (200 Å) were prepared by evaporation at 25 Å $s^{-1}$ onto glass substrates or quartz crystals. Immediately upon removal from the evaporation chamber, the metal films were immersed in a phosphate buffered saline (PBS) solution (pH = 7.4) containing 0.2 mg/mL avidin or streptavidin (Sigma) for >10 min and then washed with PBS solution to remove unbound avidin. The monolayers could be stored either dry or in buffer solutions indefinitely at 4 °C without appreciable loss of activity. Monolayers prepared on aged metal films (>1 day) exhibited lower biotin binding activities.
(6) Weber, P. C.; Ohlendorf, D. H.; Wendoloski, J. J.; Salemme, F. R. *Science* **1989**, *243*, 85-88. Molecular modeling using the known structure of the streptavidin-biotin complex indicated approximate streptavidin molecular dimensions of 42 × 42 × 56 Å. The greater thickness observed for avidin is consistent with its larger molecular weight compared to streptavidin (the proteins avidin and streptavidin exist as tetramers with molecular weights of ≈67 000 and ≈60 000, respectively).

0002-7863/90/1512-3239$02.50/0 

**Scheme I**

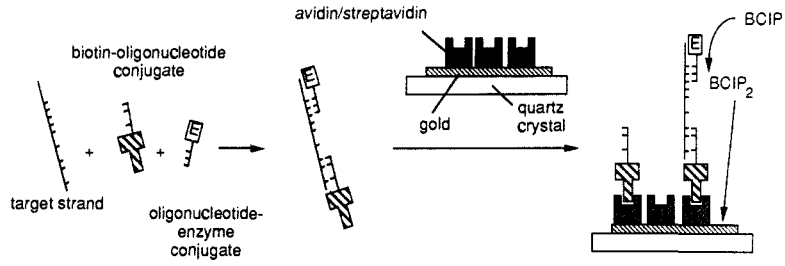


protein ionicity does not play a significant role. This implicates hydrophobic interactions or ligating functional groups ($NH_2$, $CO_2^-$) in the immobilization process. The behavior observed here appears to differ from that reported for protein adsorption on gold sols where ionic factors play a significant role.[9]

The biotin binding activities[7,10,11] of the avidin monolayers were investigated by reacting the avidin monolayers with a stoichiometric excess of biotin–alkaline phosphatase conjugate, which afforded surfaces saturated with specifically bound enzyme conjugate. The surfaces were then exposed to *p*-nitrophenyl phosphate, and the rate of enzymatic hydrolysis to *p*-nitrophenol was measured spectrophotometrically.[12] The conversion rates were $3.8 \times 10^{-10}$ and $5.3 \times 10^{-10}$ mol cm$^{-2}$ s$^{-1}$ (±5%) at 25 °C and 37 °C, respectively. Exposure of the monolayers to increasing concentrations of biotin under equilibrium conditions (>10 min) prior to the addition of biotin–alkaline phosphatase conjugate gave linearly decreasing catalytic activities. The biotin binding capacity of the monolayer is $55 \times 10^{-12}$ mol of biotin cm$^{-2}$.[13] Assuming that all four binding sites of avidin are active, this suggests a minimum avidin coverage of $14 \times 10^{-12}$ mol cm$^{-2}$, which is near the $8.3 \times 10^{-12}$ mol cm$^{-2}$ calculated for monolayer coverage.[6]

We previously reported[14] that the mass sensing capability of the quartz crystal microbalance (QCM)[15] could be exploited for detection, in solution, of alkaline phosphatase immobilized via antibody–antigen interactions on the QCM surface, on the basis of the frequency decrease (mass increase) resulting from the deposition of the 5-bromo-4-chloroindolyl phosphate (BCIP) enzymatic hydrolysis product (an insoluble dimer) onto the gold electrode surface of the QCM. Similarly, large frequency decreases were observed upon addition of BCIP to a Tris buffer solution containing an immersed QCM whose gold electrodes had been treated previously with avidin and excess biotin–alkaline phosphatase conjugate (Figure 1A). The rate of frequency change decreases with time, presumably due to accumulation of BCIP dimer on the active surface. Titration of the avidin binding sites on the QCM with biotin prior to addition of biotin–alkaline phosphatase conjugate resulted in significant decreases in the rates of frequency change as the biotin concentration was increased.

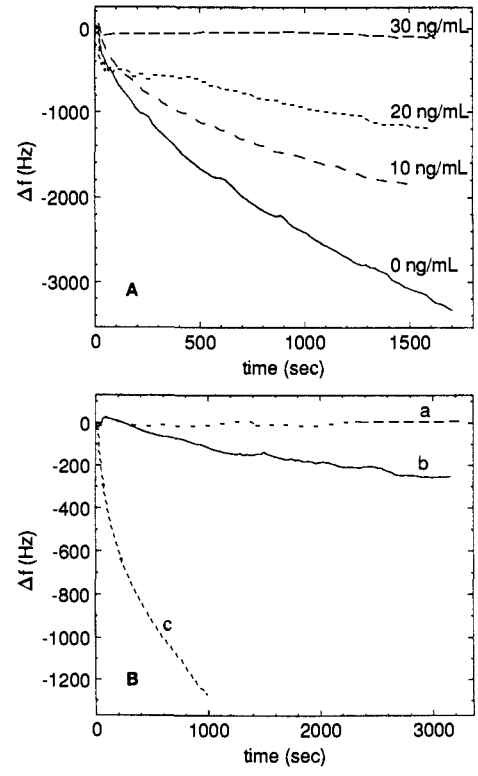


**Figure 1.** (A) QCM frequency responses upon BCIP addition at 25 °C to immobilized avidin films previously treated sequentially with various levels of biotin (as indicated) and 0.75 mg/mL biotin–alkaline phosphatase conjugate. (B) QCM responses after BCIP addition to immobilized streptavidin films treated with samples containing biotin–oligonucleotide and oligonucleotide–alkaline phosphatase probes and (a) 0 HSV-1 nucleic acid segment targets mL$^{-1}$ and (b) $2 \times 10^{11}$ HSV-1 nucleic acid segment targets mL$^{-1}$, and (c) after BCIP addition to an immobilized streptavidin film previously treated with excess biotin–alkaline phosphatase conjugate. Conditions for A and B: 50 mM Tris buffer (pH = 7.4); $1.15 \times 10^{-3}$ M BCIP.

A negligible response was detected for monolayers treated with >30 ng mL$^{-1}$ biotin, in good agreement with the *p*-nitrophenyl phosphate assays. The initial rates at 25 and 37 °C were 3.7 Hz s$^{-1}$ and 6.0 Hz s$^{-1}$, corresponding to rates of $5.0 \times 10^{-10}$ and $7.8 \times 10^{-10}$ mol of BCIP cm$^{-2}$ s$^{-1}$, respectively.

The ability to immobilize avidin on metal films makes possible a general sensor format for immunoassays and DNA probe tests, wherein the avidin monolayers provide a general capture reagent for biotinylated immunoreagents. We have demonstrated this approach by using the QCM to detect a target strand of a herpes simplex virus (HSV-1) nucleic acid (Scheme I). Probe reagents comprising biotin and alkaline phosphatase linked to separate oligonucleotide sequences, each specific for different regions of the target HSV-1 nucleic acid strand, were incubated with $2 \times 10^{11}$ targets of a HSV-1 nucleic acid segment. The hybridized target sample was then exposed to a streptavidin monolayer on a gold electrode on the QCM for 20 min. After washing of the QCM surface, BCIP was added, resulting in a frequency change of 200 Hz after 30 min due to deposition of BCIP dimer (Figure 1B). Samples without target strands did not exhibit a measurable

(7) Green, N. M. *Methods Enzymol.* **1970**, *18*, 418–424.
(8) Bonnard, C.; Papermaster, D. S.; Kraehenbuhl, J.-P. In *The streptavidin–biotin bridge technique: application in light and electron microscope immunochemistry*; Polak, J. M., Varndell, I. M., Eds.; Elsevier: Amsterdam, 1984; pp 95–111.
(9) (a) Morris, R. E.; Saelinger, C. B. *J. Microsc. (Oxford)* **1986**, *143* (Part 2), 171–176. (b) Geoghegan, W. D.; Ackerman, G. A. *J. Histochem. Cytochem.* **1977**, *25*, 1187–1200.
(10) Green, N. M. In *Avidin*; Anfinsen, C. B., Edsall, J. T., Richards, F. M., Eds.; Academic Press: New York, 1975; pp 85–133. The nearly homologous avidin and streptavidin proteins have essentially identical biotin binding affinities, with $K_D$ for the avidin–biotin complex $\approx 10^{-15}$. In our hands, there is no observable difference in the behavior of the two proteins, and the terminology avidin is used to refer to either protein, unless otherwise noted.
(11) Green, N. M. *Biochem. J.* **1966**, *101*, 774.
(12) The formation of *p*-nitrophenol was monitored at 402 nm. The *p*-nitrophenol phosphate concentration exceeded $3K_m$; see: Mukherjea, R. N.; Bhattacharya, P.; Karmakar, G. *J. Inst. Eng. (India)* **1986**, *66*, 79.
(13) This value is calculated from the total amount of biotin available in 1 mL of solution when conjugate binding was completely suppressed (15 ng/mL = $61 \times 10^{-12}$ mol, as determined by extrapolating the linear region of the response curve), the known $K_D$ for avidin–biotin, and a 1.1-cm$^2$ geometric surface area.
(14) Ebersole, R. C.; Ward, M. D. *J. Am. Chem. Soc.* **1988**, *110*, 8623.
(15) Sauerbrey, G. *Z. Phys.* **1959**, *155*, 206–222.

frequency change. Monolayers saturated with a biotin–alkaline phosphatase conjugate gave much larger frequency responses, clearly indicating that during the HSV-1 assay the streptavidin monolayer was not saturated with the HSV-1 target strand hybrid.

We have demonstrated that robust, irreversibly bound, functionally active monolayer films of avidin and streptavidin form spontaneously and rapidly on gold and silver surfaces and are useful in a broadly applicable format.

**Acknowledgment.** We thank E. Delawski, J. A. Yarem, and F. T. Gelormini for technical assistance and P. C. Weber for helpful discussions.

**Supplementary Material Available:** Complete experimental details, including procedures for the monolayer formation, biotin binding, enzymatic reactions, and HSV-1 assay (1 page). Ordering information is given on any current masthead page.

## Direct Measurement of Vibrational Temperatures in Photoexcited Deoxyhemoglobin on Picosecond Time Scales†

R. G. Alden, M. D. Chavez, and M. R. Ondrias*

*Department of Chemistry, University of New Mexico Albuquerque, New Mexico 87131*

S. H. Courtney and J. M. Friedman

*AT&T Bell Laboratories, Murray Hill, New Jersey 07974*

*Received November 30, 1989*

Recent advances in laser technology allow optical measurements, such as Raman scattering and absorption, to be performed in the picosecond and femtosecond time regimes. Commensurate with these shorter temporal regimes, the molecular dynamics of the system become increasingly complex. In addition to electronic transitions of the chromophore, the decay dynamics of photoexcited molecules are also influenced on subnanosecond time scales by the laser field impinging on the system, dielectric changes of the solvent, and conformation transitions, as well as other short-time phenomena. Power dependent broadening has been observed for the strongest Raman mode, $\nu_4$, of deoxyhemoglobin (deoxy-Hb) using 30-ps, 436-nm excitation pulses.[1] Martin and co-workers[2,3] have recently suggested that, upon absorption of a 355-nm or 580-nm photon, a vibrationally "hot" heme at 500 K results subsequent to photodissociation of CO, which cools substantially in 10 ps. Anfinrud et al.[4] have presented indirect evidence that the heme macrocycles of both deoxy-Hb and HbCO are thermally excited for 1–2 ps after photoexcitation based on base-line shifts in the free CO IR absorption region.

Classical molecular dynamics simulations have been conducted by Henry et al.,[5] to predict the rate at which excess vibrational energy in the heme is dissipated into the protein matrix for myoglobin and cytochrome *c*. In the absence of electronic radiative or nonradiative processes, the energy supplied by a 530-nm photon would result in an excess of vibrational energy and an instantaneous rise in the temperature of the porphyrin. In these heme protein systems at room temperature, complete conversion of the 530-nm photon energy equipartitioned into the vibrational modes of the ground state is estimated to raise the temperature of the heme by 500–700 K. The dissipation of the vibrational energy into the thermal bath (the protein matrix in this case) is nonexponential in time, with approximately 50% of the loss occurring in 4 ps and the remainder in 20–40 ps. Decay to the ground electronic state in deoxy-Hb occurs in <3 ps.[6] Therefore, investigation of ground-state dynamics is best addressed by utilizing 30-ps excitation pulses, which might generate steady-state populations of the putative vibrationally "hot" species.

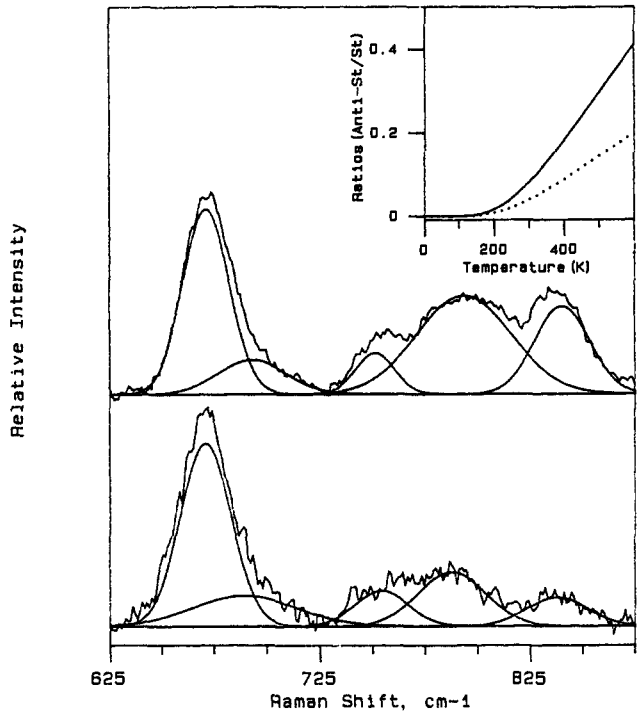


**Figure 1.** Representative 30-ps resonance Raman spectra of deoxy-Hb (pH ~7.0 in 0.1 M phosphate buffer) obtained by using 436-nm laser pulses. The 436-nm excitation wavelength was generated by anti-Stokes stimulated Raman scattering of the laser second harmonic (532 nm) of an active–passive mode-locked 30-ps Nd:YAG laser operating at 10 Hz. A spinning cell was used in all experiments to minimize the effects of photodegradation. The spectra were generated at a laser fluence of ~4 × $10^9$ W/cm$^2$. The Stokes region of the spectrum (upper spectrum) is shown from 625 to 875 cm$^{-1}$, with the fits used to extract the intensities. The bands at 671 cm$^{-1}$, 756 cm$^{-1}$, and 790 cm$^{-1}$ are $\nu_7$, $\nu_{16}$, and $\nu_{32}$, respectively, of the heme. The shoulder at ~690 cm$^{-1}$ arises from nonresonant scattering from the globin.[13] A propylene glycol mode appears at 841 cm$^{-1}$. Corresponding fits in the anti-Stokes region yield the analogous band positions and are shown in the lower spectrum. The figure shows the average fit of the 625–875-cm$^{-1}$ regions of the Stokes and anti-Stokes spectra. This yielded a ratio of 8.6% for the areas of the anti-Stokes and Stokes $\nu_7$ bands. The ratios obtained for several fits ranged from 6.7% to 10.2%. This yields temperatures of 300 ± 30 K. The variance in the ratios resulted from changes in the base-line fits and small changes in line widths of the components. The curve fits, however, are nonpathological in that only the number of lines is fixed in the calculation. The inset is a plot of the expected Boltzmann distribution for $\nu_7$ (···) in the absence of resonance and readsorption effects, while the second curve (—) displays the expected behavior of $\nu_7$ in the presence of reabsorption effects and resonance conditions at 436 nm, using the Kramers–Kronig transform technique.

Deoxyhemoglobin was chosen for this study to accentuate the effects of the vibrational population changes subsequent to absorption of a 436-nm photon. HbCO has previously been demonstrated to exhibit broadening and shifting of $\nu_4$ subsequent to CO photolysis. The phenomenon was attributed to the anharmonic coupling of $\nu_4$ to thermally populated low-frequency modes of the heme due to absorption of a 580-nm photon.[6] The resulting spectra were deconvoluted from the residual six-coordinate species and subtracted from the equilibrium deoxy-Hb spectrum to obtain the shifted and broadened $\nu_4$ spectrum. The thermal effects observed in deoxy-Hb should be larger than those in HbCO due to the

* Author to whom correspondence should be addressed.

† This work was performed at AT&T Bell Labs and was supported by the NSF (DMB 8604435) and the NIH (GM33330).

(1) Alden, R. G.; Ondrias, M. R.; Courtney, S. H.; Findsen, E. W.; Friedman, J. M. *J. Phys. Chem.* **1990**, *94*, 85.
(2) Petrich, J. W.; Martin, J. L. *Chem. Phys.* **1989**, *131*, 31.
(3) Petrich, J. W.; Martin, J. L.; Houde, D.; Poyart, C.; Orszag, A. *Biochemistry* **1987**, *26*, 7914.
(4) Anfinrud, P. A.; Han, C.; Hochstrasser, R. M. *Proc. Natl. Acad. Sci. U.S.A.* **1989**, *86*, 8397.
(5) Henry, E. R.; Eaton, W. A.; Hochstrasser, R. H. *Proc. Natl. Acad. Sci. U.S.A.* **1986**, *83*, 8982.
(6) Petrich, J. W.; Poyart, C.; Martin, J. L. *Biochemistry* **1988**, *27*, 4049.

0002-7863/90/1512-3241$02.50/0 